

REPORT 1048

A STUDY OF EFFECTS OF VISCOSITY ON FLOW OVER SLENDER INCLINED BODIES OF REVOLUTION¹

By H. JULIAN ALLEN AND EDWARD W. PERKINS

SUMMARY

The observed flow field about slender inclined bodies of revolution is compared with the calculated characteristics based upon potential theory. The comparison is instructive in indicating the manner in which the effects of viscosity are manifest.

Based on this and other studies, a method is developed to allow for viscous effects on the force and moment characteristics of bodies. The calculated force and moment characteristics of two bodies of high fineness ratio are shown to be in good agreement, for most engineering purposes, with experiment.

INTRODUCTION

The problem of the longitudinal distribution of cross force on inclined bodies of revolution in inviscid, incompressible flow, which was primarily of interest to airship designers in the past, was treated simply and effectively by Max Munk (reference 1). Munk showed that the cross force per unit length on any body of revolution having high fineness ratio can be obtained by considering the flow in planes perpendicular to the axis of revolution to be approximately two-dimensional. By treating the problem in this manner, Munk showed that

$$f = q_0 \frac{dS}{dx} \sin 2\alpha \quad (1)$$

where

- f cross force per unit length
- q_0 stream dynamic pressure
- dS/dx rate of change in body cross-sectional area with longitudinal distance along the body
- α angle of inclination

Tsien (reference 2) investigated the cross force on slender bodies of revolution at moderate supersonic speeds—a problem of more interest at the present to missile and supersonic aircraft designers—and showed that, to the order of the first power of the angle of inclination, the reduced Munk formula

$$f = 2q_0 \frac{dS}{dx} \alpha \quad (2)$$

was still applicable. This is not surprising when it is realized that the cross component of the flow field corresponds to a cross velocity

$$V_{v_0} = V_0 \sin \alpha$$

where V_0 is the stream velocity. Thus the cross component of velocity, and hence, the cross Mach number will, for small angles of inclination, have a small subsonic value so that the cross flow will be essentially incompressible in character.

Using equation (1) for the cross-force distribution, then, the total forces and moments experienced by a body in an inviscid fluid stream can be calculated. Comparison of the calculated and experimental characteristics of bodies has shown that the lift experienced exceeds the calculated lift in absolute value by an amount which is greater the greater the angle of attack; the center of pressure is farther aft than the calculations indicate, the discrepancy increasing with angle of attack; while the absolute magnitude of the moment about the center of volume is less than that calculated. It has long been known that these observed discrepancies are due primarily to the failure to consider the effects of viscosity in the flow.

Experience has demonstrated, notably in the development of airfoils, that the behavior of the boundary layer on a body is intimately associated with the nature of the pressure distribution that would exist on the body in inviscid flow. In particular, boundary-layer separation is associated with the gradient of pressure recovery on a body. The severity of the effect of such separation can be correlated, in part, with the magnitude of the total required pressure recovery indicated by inviscid theory. It is therefore to be expected that it will be of value to compare the actual pressure distribution on inclined bodies of revolution with that calculated on the assumption that the fluid is inviscid. For the purpose of this study, a simple method is developed for determining, for an inviscid fluid, the incremental pressure distribution resulting from inclined flow on a slender body of revolution.² The experimental incremental pressure distributions about an airship hull are compared with the corresponding distributions calculated by this method. The comparisons are instructive in indicating the manner in which the viscosity of the fluid influences the flow. In the light of this and other studies, a method for allowing for viscous effects on the force and moment characteristics of slender bodies is developed and the results compared with experiment.

² The problem of determining the pressure distribution on inclined bodies has been treated by other authors, but for several reasons these methods are not satisfactory for the present purposes. For example, Kaplan (reference 3) treated, in a thorough manner, the flow about slender inclined bodies, but the solution, which is expressed in Legendre polynomials, is unfortunately tedious to evaluate. On the other hand, Laftone (reference 4), by linearizing the equations of motion, obtained a solution for the pressure distribution on slender inclined bodies of revolution, but, as will be seen later, the solution is inadequate in the general case due to the linearization.

¹ Supersedes NACA TN 2044, "Pressure Distribution and Some Effects of Viscosity on Slender Inclined Bodies of Revolution" by H. Julian Allen, 1950.

SYMBOLS

A	reference area for body force and pitching-moment coefficient evaluation
A_p	plan-form area $\left(2 \int_0^L R dx\right)$
c_{d_c}	circular-cylinder section drag coefficient based on cylinder diameter
$c_{d_{\alpha=90^\circ}}$	local cross-flow drag coefficient at any x station based on body diameter
C	constant of integration
$C_{d_{\alpha=90^\circ}}$	cross-flow drag coefficient $\left(\frac{\int_0^L 2c_{d_{\alpha=90^\circ}} R dx}{A_p}\right)$
C_{D_F}	body foredrag coefficient $\left(\frac{\text{foredrag}}{q_0 A}\right)$
$C_{D_F, \alpha=0}$	body foredrag coefficient at zero angle of inclination
ΔC_{D_F}	incremental foredrag coefficient due to inclination
C_L	body lift coefficient $\left(\frac{\text{lift}}{q_0 A}\right)$
C_M	body pitching-moment coefficient about station x_m $\left(\frac{\text{pitching moment}}{q_0 A X}\right)$
D'	mean body diameter $\left(\frac{A_p}{L}\right)$
f	local cross force (normal to body axis) at any station x on body
L	body length
M_0	free-stream Mach number
M_c	cross-flow Mach number $(M_0 \sin \alpha)$
p	local surface pressure
p_0	free-stream static pressure
$p_{\alpha=0}$	local surface pressure at zero angle of inclination
P	local surface-pressure coefficient $\left(\frac{p-p_0}{q_0}\right)$
$P_{\alpha=0}$	local surface-pressure coefficient at zero angle of inclination $\left(\frac{p_{\alpha=0}-p_0}{q_0}\right)$
ΔP	incremental surface-pressure coefficient due to angle of inclination $\left(\frac{p-p_{\alpha=0}}{q_0}\right)$
q_0	free-stream dynamic pressure
Q	body volume
r	polar radius about axis of revolution
R	local body radius at any station x
R_0	free-stream Reynolds number based on maximum body diameter
R_c	cross-flow Reynolds number $(R_0 \sin \alpha)$
R_c'	cross-flow Reynolds number based on diameter D'
S	body cross-sectional area at station x

S_b	body base area (at $x=L$)
t	time
V_0	free-stream velocity
V_x	local axial velocity at body surface at any station x
V_{x_0}	axial component of the stream velocity $(V_0 \cos \alpha)$
V_{y_0}	cross-flow component of the stream velocity $(V_0 \sin \alpha)$
x	axial distance from bow of body to any body station
x_m	axial distance from bow of body to pitching-moment center
$x_{\alpha=90^\circ}$	axial distance from bow of body to center of viscous cross force
X	reference length for moment coefficient evaluation
y	ordinate in plane of inclination normal to axis of revolution
z	ordinate normal to plane of inclination and to axis of revolution
α	angle of body-axis inclination relative to free-stream-flow direction
β	$\tan^{-1} \frac{dR}{dx}$
ν	fluid kinematic viscosity
θ	polar angle about axis of revolution measured from approach direction of the cross-flow velocity
ρ	fluid mass density
ϕ	velocity potential

PRESSURE DISTRIBUTION ON SLENDER INCLINED BODIES OF REVOLUTION

POTENTIAL FLOW THEORY

Consider the flow over the body of revolution shown in figure 1, which is inclined at an angle α to the stream of velocity V_0 . If the body is slender, the axial component velocity V_x at the body surface will not differ appreciably from the axial component V_{x_0} of the stream velocity. With this condition, it is clear that the cross flow may be treated

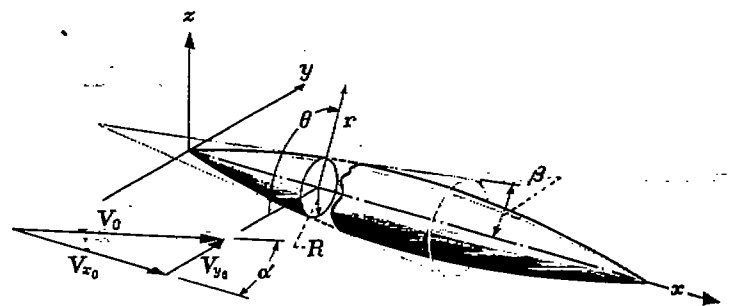


FIGURE 1.—Body of revolution in inclined flow field.

approximately by considering it to be two-dimensional in a plane which is parallel to the yz plane and is moving axially with the constant velocity V_{x_0} . In other words, the problem may be treated by determining the two-dimensional flow about a circular cylinder which is first growing (over the forebody) and then collapsing (over the afterbody) with time.

The velocity potential for the cross flow at any x station is given in polar coordinates as

$$\phi = -V_{v_0} \left(r + \frac{R^2}{r} \right) \cos \theta \quad (3)$$

which in this moving reference plane is a function of time.

Bernoulli's equation for an incompressible flow which changes with time is

$$\frac{p}{\rho} = -\frac{\partial \phi}{\partial t} - \frac{1}{2} \left[\left(\frac{\partial \phi}{\partial r} \right)^2 + \left(\frac{\partial \phi}{r \partial \theta} \right)^2 \right] + C \quad (4)$$

Now from equation (3)

$$\frac{\partial \phi}{\partial t} = -2 V_{v_0} \left(\frac{R}{r} \right) \frac{dR}{dt} \cos \theta \quad (5)$$

but

$$\frac{dR}{dt} = \frac{dx}{dt} \tan \beta = V_{x_0} \tan \beta \quad (6)$$

so that equation (5) becomes

$$\frac{\partial \phi}{\partial t} = -2 V_{v_0} V_{x_0} \tan \beta \left(\frac{R}{r} \right) \cos \theta \quad (7)$$

Also, by differentiation of equation (3),

$$\left. \begin{aligned} \frac{\partial \phi}{\partial r} &= -V_{v_0} \cos \theta \left(1 - \frac{R^2}{r^2} \right) \\ \frac{\partial \phi}{r \partial \theta} &= V_{v_0} \sin \theta \left(1 + \frac{R^2}{r^2} \right) \end{aligned} \right\} \quad (8)$$

so that equation (4) for the pressure at any point in the flow field becomes

$$\frac{p}{\rho} = 2 V_{v_0} V_{x_0} \tan \beta \left(\frac{R}{r} \right) \cos \theta - \frac{V_{v_0}^2}{2} \left\{ \cos^2 \theta \left[1 - \left(\frac{R}{r} \right)^2 \right]^2 + \sin^2 \theta \left[1 + \left(\frac{R}{r} \right)^2 \right]^2 \right\} + C \quad (9)$$

For

$$r \rightarrow \infty, p \rightarrow p_0$$

so

$$C = \frac{p_0}{\rho} + \frac{V_{v_0}^2}{2}$$

and hence equation (9) for the pressure at the surface of the body becomes for $r=R$

$$\frac{p-p_0}{\rho} = 2 V_{v_0} V_{x_0} \tan \beta \cos \theta + \frac{V_{v_0}^2}{2} (1-4 \sin^2 \theta) \quad (10)$$

and writing

$$V_{v_0} = V_0 \sin \alpha$$

$$V_{x_0} = V_0 \cos \alpha$$

the surface pressure in coefficient form becomes

$$P = \frac{p-p_0}{q_0} = 2 \tan \beta \cos \theta \sin 2\alpha + (1-4 \sin^2 \theta) \sin^2 \alpha \quad (11)$$

For bodies of moderate fineness ratio at zero angle of inclination, the surface pressure at any station, designated $p_{\alpha=0}$, will differ slightly from the static pressure p_0 but, if the fineness ratio is not too low, the pressure, $p_{\alpha=0}$, in any yz plane will be approximately constant for several body radii from the surface. Under the assumption that the pressure at the surface at zero inclination applies uniformly in the portion of the yz plane for which the major effects of the cross-flow distribution are felt, the change in pressure from p_0 to $p_{\alpha=0}$ will be additive to, but will not otherwise influence, the cross-flow pressure distribution. Hence for any station on a body of high fineness ratio for which at zero inclination the pressure is $p_{\alpha=0}$, the pressure coefficient distribution at this same station under inclined flow conditions will be, from equation (11),

$$P = P_{\alpha=0} + (2 \tan \beta \cos \theta) \sin 2\alpha + (1-4 \sin^2 \theta) \sin^2 \alpha \quad (12)$$

For very slender bodies at small angles of inclination

$$\tan \beta \cong \beta$$

$$\sin 2\alpha \cong 2\alpha$$

$$\sin^2 \alpha \cong \alpha^2$$

so that equation (12) becomes³

$$P = P_{\alpha=0} + (4 \cos \theta) \beta \alpha + (1-4 \sin^2 \theta) \alpha^2 \quad (13)$$

The cross force per unit length of the body is then found as

$$f = \int_0^{2\pi} p R \cos \theta d\theta = 2 q_0 \int_0^\pi P R \cos \theta d\theta + 2 \int_0^\pi p_0 R \cos \theta d\theta$$

³ Equation (13), for the case in which β is constant, reduces to that derived by Busemann (reference 5) for the flow over an inclined cone. Laltone's linearized solution (reference 4) for the pressure distribution over bodies at supersonic speeds agrees with equation (13) except that the α^2 term, of course, is absent. This linearized solution is inadequate in general since, for the cases of usual interest, the values of α are of the same order of magnitude as β , thus the α^2 term is as important as the α term.

and clearly

$$2 \int_0^\pi p_0 R \cos \theta d\theta = 0$$

Substituting P from equation (12) gives

$$f = 2Rq_0 P_{\alpha=0} \int_0^\pi \cos \theta d\theta + 4Rq_0 \tan \beta \sin 2\alpha \int_0^\pi \cos^2 \theta d\theta + 2Rq_0 \sin^2 \alpha \int_0^\pi (1 - 4 \sin^2 \theta) \cos \theta d\theta$$

The first and third integrals are zero, while the second integral yields

$$f = 2\pi R q_0 \tan \beta \sin 2\alpha$$

and since

$$2\pi R \tan \beta = 2\pi R \frac{dR}{dx} = \frac{dS}{dx}$$

then

$$f = q_0 \frac{dS}{dx} \sin 2\alpha$$

which is equation (1) derived by Munk for the cross force on slender airship hulls and, in the form,

$$f = 2q_0 \frac{dS}{dx} \alpha$$

that derived by Tsien for the cross force, to the order of the first power of the angle of inclination, for slender bodies at moderate supersonic speeds. This development shows that these equations for the cross force are also correct to the second power of α for inviscid flow.

COMPARISONS WITH EXPERIMENT AND DISCUSSION OF THE EFFECTS OF VISCOSITY

In reference 6, a thorough investigation at low speeds was made of the pressure distribution over a hull model of the rigid airship "Akron." Incremental pressure distributions due to inclination calculated by equation (12) for four stations along the hull at three angles of attack are compared with the experimental values in figures 2(a) to 2(d). In each of the figures is shown a sketch of the airship which indicates the station at which the incremental pressure distributions apply. This comparison represents a severe test of the theoretical method of this report since the method was developed on the assumption that the fineness ratio of the body is very large, while for the case considered the fineness ratio is only 5.9.

At the more forward stations (figs. 2(a) and 2(b)), the agreement is seen to be essentially good⁴ but some discrep-

⁴ At stations extremely close to the bow the method must be inaccurate as evident from the work of Upson and Kilkoiff (reference 7).

ancy, particularly at values of θ near 180° , is evident which increases with increasing distance from the bow. Downstream of the maximum diameter section (figs. 2(c) and 2(d)) the discrepancy increases very rapidly.

The disagreement that exists at the afterbody stations results from effects of viscosity not considered in the theory, as will be seen from the following: R. T. Jones, in reference 8, showed that, for laminar flow on an infinitely long yawed cylinder of arbitrary cross section, the behavior of the component flow of a viscous fluid in planes normal to the cylinder axis was independent of the component flow parallel to the axis.⁵ For an inclined circular cylinder, then, viewed along the cylinder axis the viscous flow about the cylinder would appear identical to the flow about a circular cylinder section in a stream moving at the velocity $V_\infty \sin \alpha$. Hence separation of the flow would occur in the yz plane as a result of the adverse pressure gradients that exist across the cylinder. Jones demonstrated that this behavior explained the cross forces on inclined right circular cylinders that were experimentally observed in reference 10. That such separation effects also occur on the inclined hull model of the "Akron" is also evident from the pressure distributions in figures 2(c) and 2(d).

While the treatment of reference 8 explains qualitatively the observed behavior of the flow field about the hull model considered, it cannot be used quantitatively for a low fineness ratio body such as the "Akron" for at least two reasons. First, the influence of the term

$$2 \tan \beta \cos \theta \sin 2\alpha$$

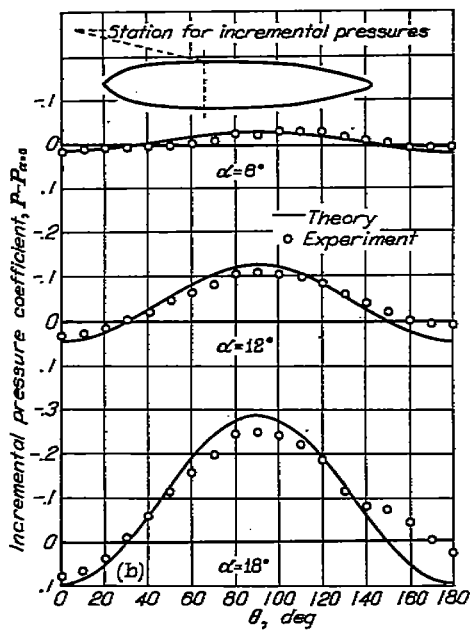
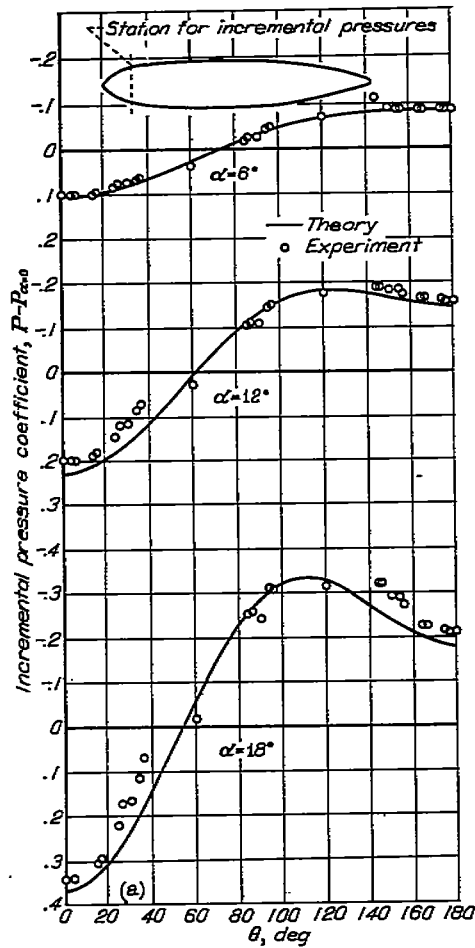
of equation (12) is to distort the typical circular-cylinder pressure distribution, given by the term

$$(1 - 4 \sin^2 \theta) \sin^2 \alpha$$

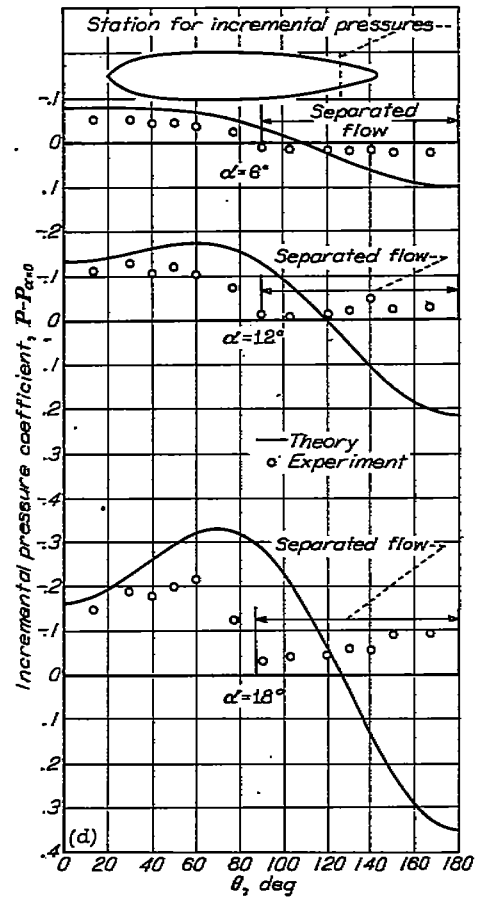
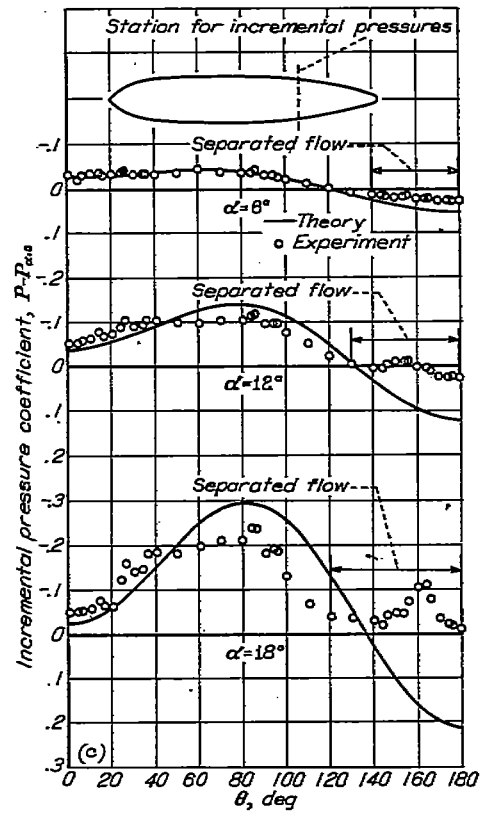
so as to move the calculated position of minimum pressure away from the $\theta = 90^\circ$ point and to change the magnitude of the pressure to be recovered on the lee side of the body. Over the forward stations of the body, where $\tan \beta$ is positive, the position of minimum pressure lies between 90° and 180° and the theoretical pressure recovery is small and even zero at the most forward stations. For the rearward station where $\tan \beta$ is negative, the minimum pressure lies between 0° and 90° , and the theoretical pressure recovery is large and increases proceeding toward the stern. For the hull of the "Akron" model, the theoretical line of minimum pressure along the hull is shown in figure 3 for the angles of attack of 6° , 12° , and 18° .⁶ Since separation can only occur in an adverse

⁵ The recent work of A. P. Young and T. B. Booth (reference 9) indicated that this may be true for the turbulent flow case as well.

⁶ It is of interest to note in this figure that even for small angles of inclination the line of minimum pressure becomes oriented close to the direction of the axis of revolution, while at zero inclination it must, of course, be normal to this axis.



(a) $z/L = 0.111$;
(b) $z/L = 0.355$;



(c) $z/L = 0.708$;
(d) $z/L = 0.867$.

FIGURE 2—Calculated and experimental pressure distribution on a model hull of the U. S. S. Akron.

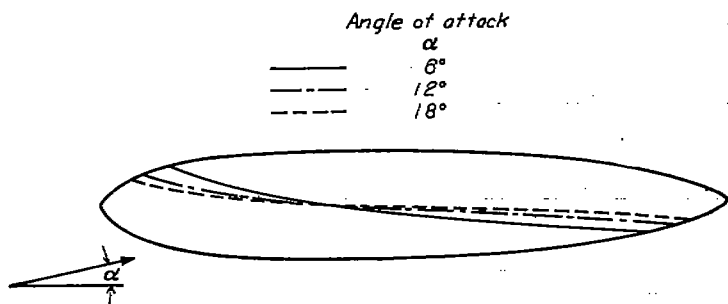


FIGURE 3.—Calculated lines of minimum pressures for a model hull of U. S. S. Akron at three angles of attack.

gradient, it is clear that the line of separation will roughly parallel the line of minimum pressures. Hence, the flow about forward stations will be, or will more nearly be, that calculated for a nonviscous fluid. Over the rearward stations the flow separation should tend to be even more pronounced than would occur on a right circular cylinder. That such is the case is shown by the flow studies on the ellipsoid of revolution of reference 11. In those studies, the flow on the model surface was investigated by lampblack and kerosene traces. The traces showed the line of separation followed the trend indicated above. From the foregoing, it is evident that the potential flow solution for the pressures on inclined bodies can only be expected to hold over the forebody, and that over the afterbody the pressure distribution, particularly on the lee side, will be importantly influenced by the fluid viscosity.

Second, it is evident that there exists a certain analogy between the cross flow at various stations along the body and the development with time of the flow about a cylinder starting from rest. This may be seen by considering the development of the cross flow with respect to a coordinate system that is in a plane perpendicular to the axis of the inclined body. Let the plane move downstream with a velocity V_0 and let the coordinate system move within the plane such that the axis of revolution of the body is always coincident with the x axis of the coordinate system. The cross velocity is then $V_0 \sin \alpha$. At any instant during the travel of the plane from the nose to the base of the body, the trace of the body in the plane will be a circle and the cross-flow pattern within the plane may be compared with the flow pattern about a circular cylinder. Neglecting, for the moment, the effect of the taper over the nose portions of the body, it might be anticipated that over successive downstream sections, the development of the cross flow with distance along the body as seen in this moving plane would appear similar to that which would be observed with the passage of time for a circular cylinder impulsively set in motion from rest with the velocity $V_0 \sin \alpha$. Thus the flow in the cross plane for the more forward sections should contain a pair of symmetrically disposed vortices on the lee side (cf. reference 12). These vortices should increase in strength as the plane moves rearward and eventually, if the body is long enough, should discharge to form a Kármán vortex street as viewed in the moving cross plane. Viewed in

this moving plane the vortices would appear to be shed and slip rearward in the wake, but viewed with respect to the stationary body the shed vortices would appear fixed. This process of the growth and eventual discharge of the lee-side vortices should occur over a shorter length of body the higher the angle of attack since the movement of the cylindrical trace in the cross plane at any given station is greater the greater the angle of attack. For a low fineness ratio body, however, the development of the lee-side vortices would be expected to have progressed no farther than the "symmetrical pair" case even at the highest angles of attack of interest. This is corroborated by the flow surveys of Harrington (reference 11).

For bodies of high fineness ratio, such as those used for supersonic missiles, it was clearly of interest to determine experimentally the nature of the anticipated growth and discharge of lee-side vortices. In the course of an investigation of a series of bodies with ogival noses and cylindrical afterbodies conducted in the Ames Laboratory 1- by 3-foot supersonic wind tunnels, it was determined that the growth and discharge of lee-side vortices did occur for such bodies at angle of attack as was evidenced in two ways. The schlieren picture for one of the bodies (fig. 4 (a)) showed a line on the lee side at the more forward stations which drifted away from the body surface and eventually branched into a series of lines trailing in the stream direction. The "line" at the more forward stations was indicated to be the cores of the symmetrical vortex pair, which in this side view would appear coincident. The branches were indicated to be the cores of the alternately shed vortices. In order to make the vortices visible in a more convincing manner, use was made of a technique which we have termed the "vapor screen" method. With this technique, the cross flow is made visible in the following manner (see fig. 5): A small amount of water vapor, which condenses in the wind-tunnel test section to produce a fine fog, is introduced into the tunnel air stream. A narrow plane of bright light, produced by a high-pressure mercury-vapor lamp, is made to shine through the glass window in a plane essentially perpendicular to the axis of the tunnel. In the absence of the model this plane appears as a uniformly lighted screen of fog particles. When the model is put in place at any arbitrary angle of attack, the result of any disturbances in the flow produced by the model which affects the amount of light scattered by the water particles in this lighted plane can be seen and photographed.

In figures 4 (b) and 4 (c) are shown photographs of the vapor screens corresponding to the indicated stations for the body of figure 4 (a). The photographs are three-quarter front views from a vantage point similar to that of the sketch of figure 5. In these photographs vortices made themselves evident as black dots on the vapor screens due to the absence of scattered light, which is believed to result from the action of the vortices in spinning the fine droplets of fog out of the fast turning vortex cores. Other details of the flow, particu-

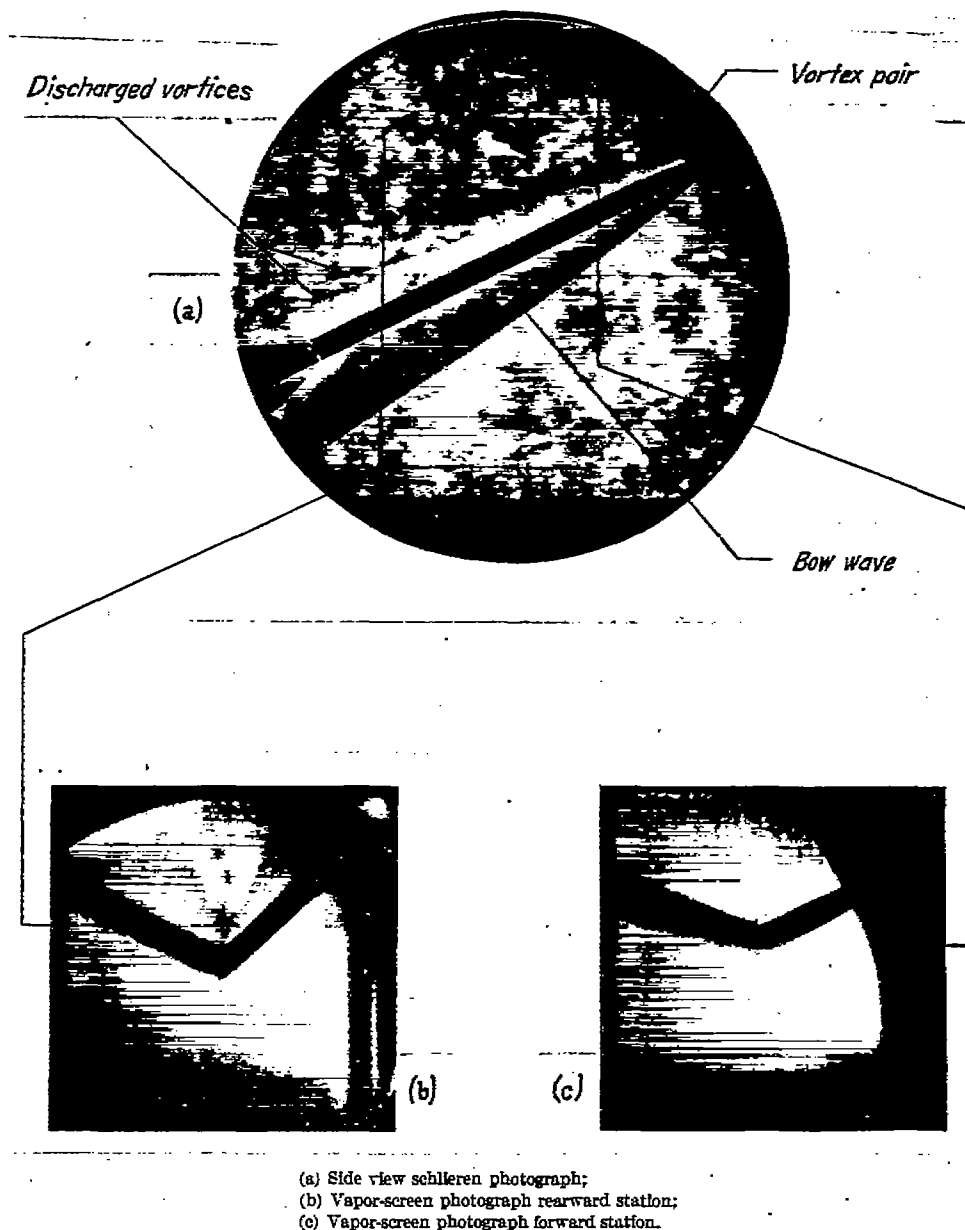


FIGURE 4.—Schlieren and vapor-screen photographs showing vortex configuration for an inclined body of revolution ($\alpha \approx 25^\circ$) at supersonic speed ($M \approx 2$).

larly shock waves, are evident as a change in light intensity. Figure 4 (c) shows the symmetrical vortex pair to exist as previously indicated at the more forward stations, while figure 4 (b) demonstrates that the vortices are shed at stations far removed from the bow. Other observations at different angles of attack demonstrated that the shedding of vortices began, as indicated previously, at the more forward stations the higher the angle of attack. It is of interest to point out that in these wind-tunnel tests the order of discharge of the vortices was aperiodically reversed. Thus, in any cross-flow plane, the discharged vortex closest to the body would at one instant be on one side of the body and at the next instant, or perhaps several seconds later, on the other. No regularity in this change in the distribution of the vortex street has been found.

METHOD FOR ESTIMATING FORCE AND MOMENT CHARACTERISTICS OF SLENDER INCLINED BODIES IN VISCOUS FLOW

For bodies of high fineness ratio at high angles of attack when the cross force is important, it is clear that the third term of equation (13) must predominate since β is small, so that the pressure distribution increment due to angle of attack will closely approximate the pressure distribution for a circular-cylinder section at a velocity equal to the cross component of velocity for the body. Moreover, except for the sections near the bow, development of the cross-flow boundary layer will have been sufficient to promote the flow that is characteristic of the steady-state flow for a circular-cylinder section at the Mach and Reynolds numbers corresponding to the cross velocity over the body.

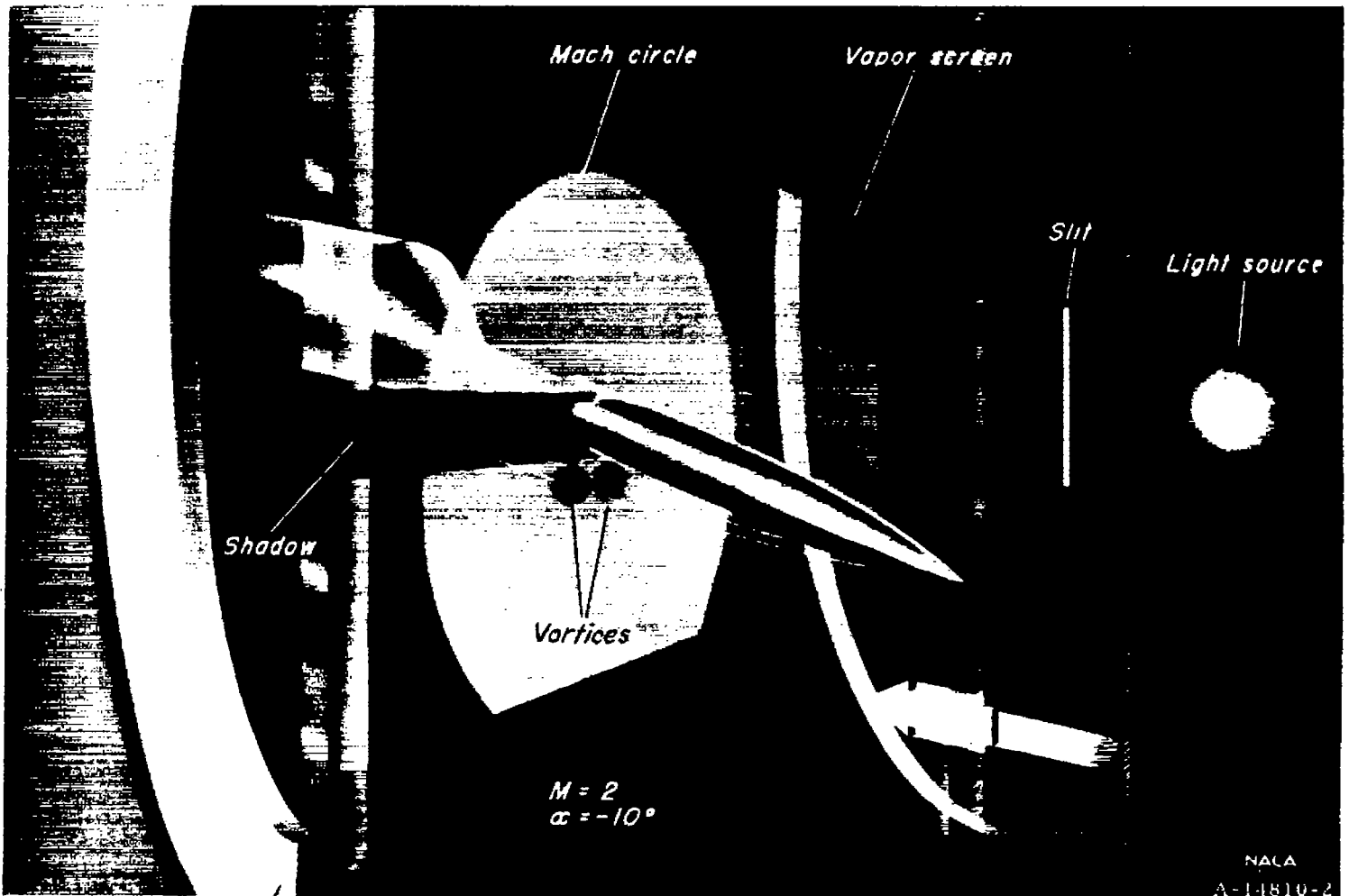


FIGURE 5.—Schematic diagram of vapor-screen apparatus showing vortices from a lifting body of revolution.

For the limiting case of a slender body, the appropriate value of the cross-wise drag coefficient is, of course, the value of the drag for an infinite cylinder. As will be shown later, experiments indicate that for actual bodies of finite length a somewhat smaller value should be used. Since the actual cross-wise drag coefficient of a body of finite length is always somewhat less than the coefficient for an infinite body, this reduced value suggests itself. Thus it might be expected that the viscous cross-force distribution on such a body could be calculated on the assumption that each circular element along the body experiences a cross force equal to the drag force the section would experience with the axis of revolution normal to a stream moving at the velocity $V_0 \sin \alpha$. This viscous contribution is given by

$$2Rc_{d\alpha=90^\circ} q_0 \sin^2 \alpha dx$$

where R is the body radius at x and $c_{d\alpha=90^\circ}$ is the local drag

coefficient at x for $\alpha=90^\circ$ corresponding to the Reynolds number

$$R_c = R_0 \sin \alpha$$

and the Mach number

$$M_c = M_0 \sin \alpha$$

As a first approximation to the total cross force we may add the potential cross force to the viscous contribution. The total cross force at x would then be ⁷

$$f = q_0 \frac{dS}{dx} \sin 2\alpha \cos \frac{\alpha}{2} + 2Rc_{d\alpha=90^\circ} q_0 \sin^2 \alpha$$

With this simple allowance for viscous effects the lift coefficient,⁸ the foredrag coefficient, and the pitching-moment

⁷ From the work of Ward (reference 13), it may be shown that the potential cross force is directed midway between the normal to the axis of revolution and the normal to the wind direction.

⁸ In the expression for C_L the contribution of the axial drag force $-C_{D_p}(\alpha=0) \cos^2 \alpha \sin \alpha$ is inconsequentially small and has been ignored.

coefficient about an arbitrary moment center x_m from the nose are given by

$$\left. \begin{aligned} C_L &= \frac{S_b}{A} \sin 2\alpha \cos \frac{\alpha}{2} + C_{d_{\alpha=90^\circ}} \frac{A_p}{A} \sin^2 \alpha \cos \alpha \\ C_{D_F} &= C_{D_{F_{\alpha=0}}} \cos^3 \alpha + \frac{S_b}{A} \sin 2\alpha \sin \frac{\alpha}{2} + C_{d_{\alpha=90^\circ}} \frac{A_p}{A} \sin^3 \alpha \\ C_M &= \left[\frac{Q - S_b(L - x_m)}{AX} \right] \sin 2\alpha \cos \frac{\alpha}{2} + \\ & C_{d_{\alpha=90^\circ}} \frac{A_p}{A} \left(\frac{x_m - x_{\alpha=90^\circ}}{X} \right) \sin^2 \alpha \end{aligned} \right\} (14)$$

where

$$C_{d_{\alpha=90^\circ}} = \frac{\int_0^L c_{d_{\alpha=90^\circ}} 2R dx}{A_p}$$

and

$$x_{\alpha=90^\circ} = \frac{\int_0^L c_{d_{\alpha=90^\circ}} 2R x dx}{A_p C_{d_{\alpha=90^\circ}}}$$

where

- A_p plan-form area
- S_b base area
- Q body volume
- L body length
- A reference area for coefficient evaluation
- X reference length for pitching-moment-coefficient evaluation

Because of the approximate nature of the theory, it is not considered justified to retain the complex forms of these equations. Accordingly, it is assumed that, for the functions of the angle of attack, cosines may be replaced by unity and sines by the angles in radians to give⁹

$$\left. \begin{aligned} C_L &= 2 \left(\frac{S_b}{A} \right) \alpha + C_{d_{\alpha=90^\circ}} \left(\frac{A_p}{A} \right) \alpha^2 \\ \Delta C_{D_F} &= C_{D_F} - C_{D_{F_{\alpha=0}}} = \frac{S_b}{A} \alpha^2 + C_{d_{\alpha=90^\circ}} \left(\frac{A_p}{A} \right) \alpha^2 \\ C_M &= 2 \left[\frac{Q - S_b(L - x_m)}{AX} \right] \alpha + C_{d_{\alpha=90^\circ}} \left(\frac{A_p}{A} \right) \left(\frac{x_m - x_{\alpha=90^\circ}}{X} \right) \alpha^2 \end{aligned} \right\} (15)$$

To assess the adequacy of these equations for predicting the force and moment characteristics of high fineness ratio bodies, two bodies of revolution were tested in the 1- by 3-foot supersonic wind tunnel at a Mach number of 1.98 from angles of attack of zero to more than 20° and in the 1- by 3½-foot high-speed wind tunnel from Mach numbers of 0.3 to 0.7 at 90° angle of attack to determine the cross-flow drag coefficient $C_{d_{\alpha=90^\circ}}$ and the center of application $x_{\alpha=90^\circ}$ of this force.¹⁰ The bodies investigated (see fig. 6)

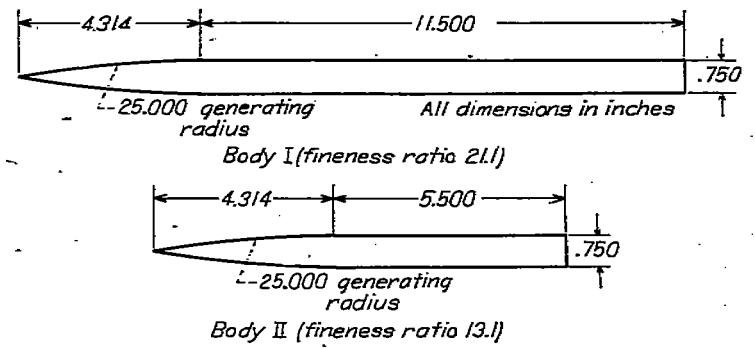


FIGURE 6.—Bodies of revolution.

each had a 33¼-caliber ogival nose and constant diameter afterbody of such length as to make the fineness ratios 21.1 for body I and 13.1 for body II. Shown in figures 7 and 8 are the lift coefficient, foredrag-increment coefficient, pitching-moment coefficient about the bow, and center of pressure as a function of angle of attack for the two bodies as determined from the tests in the 1- by 3-foot wind tunnels. Also shown are the calculated characteristics (indicated by the solid-line curves) using the experimental values of $C_{d_{\alpha=90^\circ}}$ and $x_{\alpha=90^\circ}$ (see figs. 9 and 10) obtained from the 90° angle-of-attack tests in the 1- by 3½-foot wind tunnel as well as calculated characteristics obtained from potential theory (indicated by the dotted-line curves). The reference area A for coefficient evaluation for these data is the base area and the reference length X for moment-coefficient evaluation is the base diameter.

It is seen that for the higher fineness ratio body (body I), the calculated characteristics which include the allowance for viscous effects are in good agreement with experiment and that the potential theory is clearly inadequate at all but very small angles of attack. For the lower fineness ratio body (body II), the calculated allowances for viscous effects depart further from experiment than they do for body I, as would be expected, although again they are in much better agreement with experiment than are the calculated characteristics based only on potential theory.

While the comparisons made demonstrate that the indicated allowance for viscous effects is adequate for very high-fineness-ratio bodies, the calculated characteristics were, themselves, based on experimentally determined values of $C_{d_{\alpha=90^\circ}}$ and $x_{\alpha=90^\circ}$. For the method to be useful in design, of course, some means for calculating these parameters must exist. In many cases, there are available sufficient experimental drag data on cylinders to provide the required information. In the appendix one approximate method is given for determining the values of $C_{d_{\alpha=90^\circ}}$ and $x_{\alpha=90^\circ}$ for the bodies I and II previously considered.

The variations of the coefficients of lift, foredrag increment, and pitching moment and of the center-of-pressure position with angle of attack for the two bodies as estimated using the calculated cross-flow drag characteristics given in the appendix are shown in figures 7 and 8 (as the dashed-line curves). The estimated characteristics are seen to be in even better agreement with experiment than are the calculated variations using the experimental cross-flow drag characteristics.

⁹ In the expression for ΔC_{D_F} , the term $-C_{D_{F_{\alpha=0}}} \alpha^2$, which should properly appear on the right side of this equation, has been omitted since, for practical cases, its contribution is small.

¹⁰ Although the cross Reynolds numbers for the 1- by 3½-foot wind-tunnel test were almost twice that for the 1- by 3-foot wind-tunnel tests, the results are considered comparable since in the range of Reynolds numbers investigated the drag characteristics of circular cylinders are insensitive to change in Reynolds numbers.

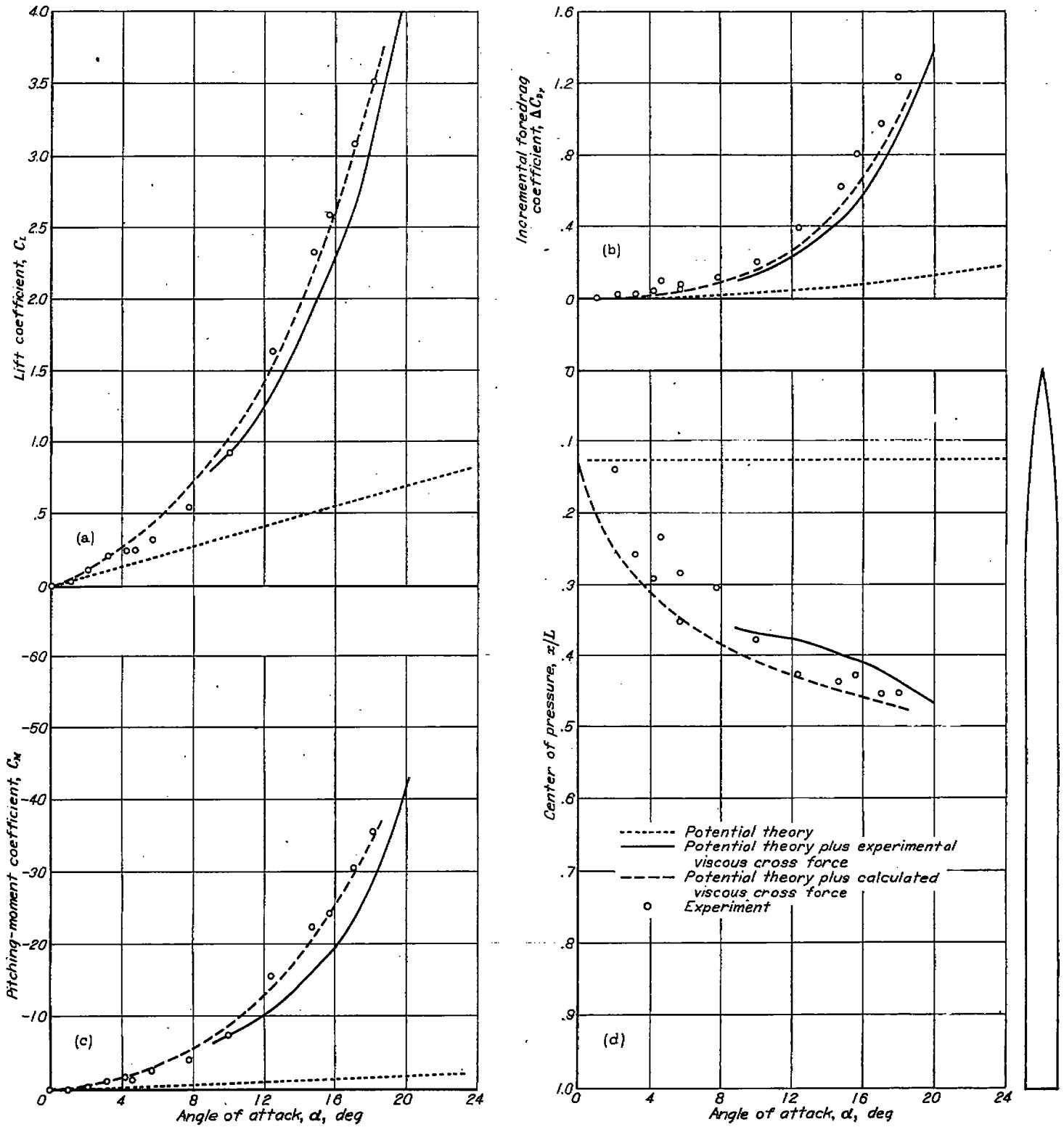


FIGURE 7.—Force, moment, and center-of-pressure characteristics for body I (fineness ratio 21.1).

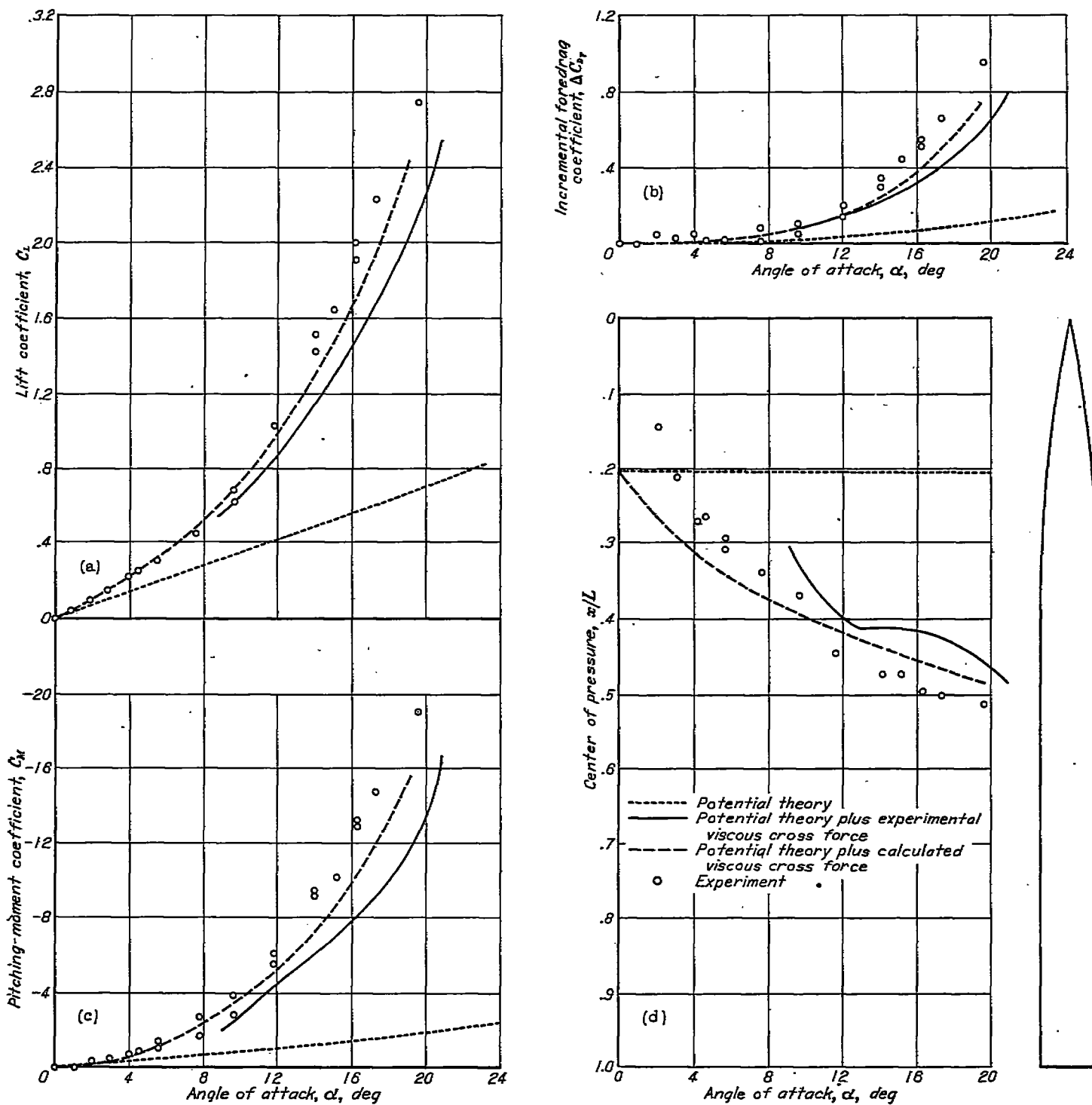


FIGURE 8.—Force, moment, and center-of-pressure characteristics for body II (fineness ratio 18.1).

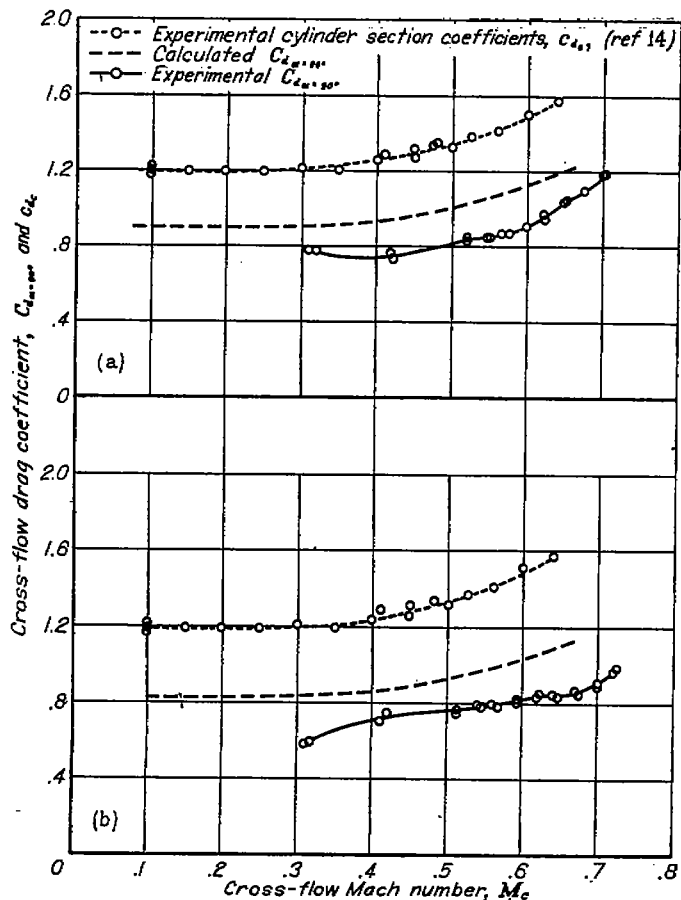


FIGURE 9.—Comparison of calculated cross-flow drag coefficients at 90° angle of attack with experimental values obtained from Ames 1-by 3¼-foot wind tunnel for (a) body I and (b) body II.

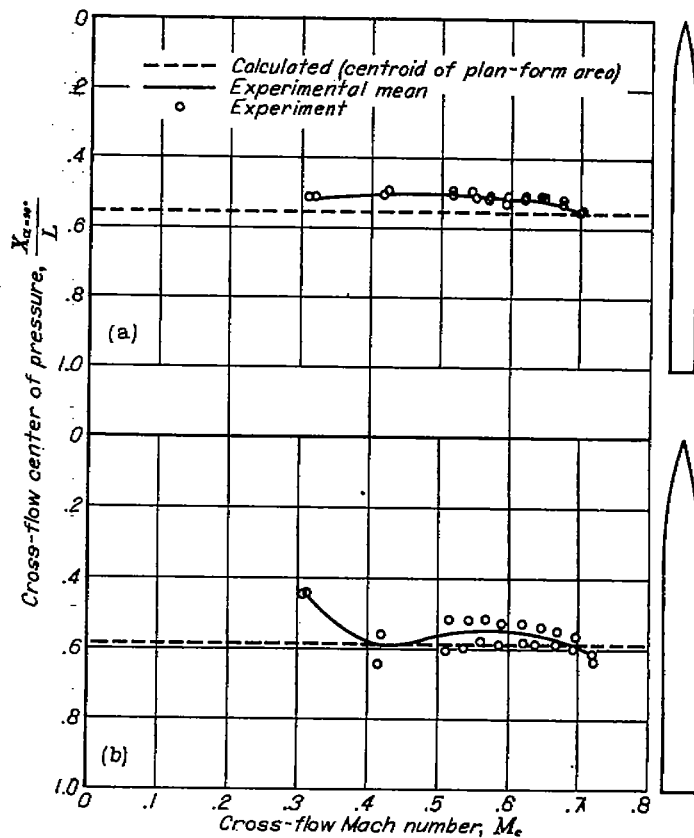


FIGURE 10.—Comparison of calculated centers of pressure at 90° angle of attack with experimental values obtained from Ames 1-by 3¼-foot wind tunnel for (a) body I and (b) body II.

AMES AERONAUTICAL LABORATORY,
 NATIONAL ADVISORY COMMITTEE FOR AERONAUTICS,
 MOFFETT FIELD, CALIF., Dec. 28, 1949.

APPENDIX

ESTIMATION OF CROSS-FLOW DRAG COEFFICIENT

A procedure which suggests itself for estimating the magnitude of the cross-flow drag coefficient $C_{d_{\alpha=90^\circ}}$ as a function of angle of attack for the two ogival-nosed bodies treated in the text is to consider them to have the same characteristics as circular cylinders of constant diameter.

$$D' = \frac{A_p}{L}$$

The cross-flow drag coefficient of this fictitious cylinder of finite length can then be approximated by first determining the drag coefficient, c_{d_c} , of a circular-cylinder section of diameter D' at the cross-flow Mach number

$$M_c = M_0 \sin \alpha$$

and cross-flow Reynolds number

$$R_c' = \frac{V_0 D'}{\nu} \sin \alpha$$

and then correcting this drag coefficient for the effect of the finite fineness ratio, L/D' .

From references 14 and 15, it is found that for the values of D' corresponding to the two bodies considered the circular-cylinder section drag coefficients, c_{d_c} , are the same for both bodies and dependent only on the Mach number. The values at various cross Mach numbers are given in figure 9.

From reference 16, it is found that for a finite-length circular cylinder in the range of Reynolds numbers for which the cross-drag coefficient, as for the present cases, is 1.2 at low Mach numbers, the ratio of the drag of the circular cylinder of finite length to that for the circular cylinder of infinite length is 0.755 for body I and 0.692 for body II. Assuming that this ratio is independent of Mach number, the estimated values of $C_{d_{\alpha=90^\circ}}$ for the two bodies are as given in figure 9 wherein they may be compared with the experimental values obtained from the 1- by 3½-foot wind-tunnel tests.

The value of $x_{\alpha=90^\circ}$ is logically assumed to be the distance from the bow to the centroid of plan-form area. This

assumed position which is independent of Mach number is compared with the experimentally determined values from the 1- by 3½-foot wind-tunnel tests for the two bodies in figure 10.

REFERENCES

1. Munk, Max M.: The Aerodynamic Forces on Airship Hulls. NACA Rep. 184, 1924.
2. Tsien, Hsue-Shen: Supersonic Flow Over an Inclined Body of Revolution. Jour. Aero. Sci., vol. 5, no. 12, Oct. 1938, pp. 480-483.
3. Kaplan, Carl: Potential Flow About Elongated Bodies of Revolution. NACA Rep. 516, 1935.
4. Laitone, E. V.: The Linearized Subsonic and Supersonic Flow About Inclined Slender Bodies of Revolution. Jour. Aero. Sci., vol. 14, no. 11, Nov. 1947, pp. 631-642.
5. Busemann, Adolf: Infinitesimal Conical Supersonic Flow. NACA TM 1100, 1947.
6. Freeman, Hugh B.: Pressure-Distribution Measurements on the Hull and Fins of a 1/40-Scale Model of the U. S. Airship "Akron." NACA Rep. 443, 1932.
7. Upson, Ralph H., and Klikoff, W. A.: Application of Practical Hydrodynamics to Airship Design. NACA Rep. 405, 1931.
8. Jones, Robert T.: Effects of Sweepback on Boundary Layer and Separation. NACA Rep. 884, 1947. (Formerly NACA TN 1402)
9. Young, A. D., and Booth, T. B.: The Profile Drag of Yawed Wings of Infinite Span. The College of Aeronautics, Cranfield. Rep. 38, May, 1950.
10. Relf, E. F. and Powell, C. H.: Tests on Smooth and Stranded Wires Inclined to the Wind Direction, and a Comparison of Results on Stranded Wires in Air and Water. R. & M. No. 307, British A. R. C., 1917.
11. Harrington, R. P.: An Attack on the Origin of Lift of an Elongated Body. Daniel Guggenheim Airship Inst., Publication 2, 1935.
12. Schwabe, M.: Pressure Distribution in Nonuniform Two-Dimensional Flow. NACA TM 1039, 1943.
13. Ward, G. N.: Supersonic Flow Past Slender Pointed Bodies. Quar. Jour. of Mech. and Applied Math., vol. 2, part I, Mar. 1949, pp. 75-97.
14. Lindsey, W. F.: Drag of Cylinders of Simple Shapes. NACA Rep. 619, 1938.
15. Stack, John: Compressibility Effects in Aeronautical Engineering. NACA ACR, Aug. 1941.
16. Goldstein, S.: Modern Developments in Fluid Dynamics. Oxford, The Clarendon Press, 1938, vol. II, pp. 419-421.